

## Dynamic Structure Optimization Design of Lower Control Arm Based on ESL

<sup>1,2</sup>Lihui Zhao, <sup>1,3</sup>Songlin Zheng, <sup>1,3</sup>Jinzhi Feng and <sup>4</sup>Qingquan Hong

<sup>1</sup>College of Mechanical Engineering, University of Shanghai for Science and Technology,  
Shanghai 200093, PR China

<sup>2</sup>Automotive Engineering College, Shanghai University of Engineering Science,  
Shanghai 201620, PR China

<sup>3</sup>Machinery Industry Key Laboratory for Mechanical Strength and Reliability Evaluation of Auto  
Chassis Components, Shanghai 200093, PR China

<sup>4</sup>Altair Engineering Software (Shanghai) Co., Ltd., Shanghai 200093, China

**Abstract:** Structure optimization techniques under static load conditions have been widely used in automotive industry for lightweight and performance improvement of modern cars. However, these static load conditions could not represent all the severe situations of automobile parts which subjected to complex loads varying with time, especially for lower control arm of front suspension. In this study, dynamic optimization of lower control arm was performed by combining traditional static load optimization techniques and multi-body dynamics by Equivalent Static Load (ESL). And the best draw-bead distribution of the stamped lower control arm was attained. Comparing the MBD analysis results of the new design derived from dynamic optimization and original structure, results show that the strength and stiffness was increased significantly while the mass was almost unchanged.

**Keywords:** Double-wishbone suspension, dynamic optimization, equivalent static load, lower control arm

### INTRODUCTION

The lower control arm was a key part of front suspension which controls the wheel trace and transmits load exerting on the wheel by the road to other parts of the car. When the car was running on the road, the lower control arm was subjected to complex loads alternating with time. Thus, the mechanical performances, usually relating to strength and stiffness were critical to the safety and reliability of the car. Recently, many analysis and optimization methods and tools for structure design based on CAE have been introduced into automobile industry. Most of them were based on static load conditions, which were derived from multi-body dynamic analysis or experimental tests (Pan, 2007; Fu, 2009; Wang, 2009; Lu, 2011).

However, accurately obtaining the static load conditions exist two key issues:

- A large number of analyses on load history should be done, which requires engineers' experience
- Constraints at different time were different due to the different motion state of the parts

This made engineers spending lots of time in analyzing and extracting the correct load and boundary conditions and finally increased the developing cycle of automobile products. In this study, optimization of

draw-bead distribution of lower control arm under dynamic load conditions was applied by combining the traditional optimization techniques and flexible multi-body dynamic analysis by equivalent static load method (Kang *et al.*, 2001; Park and Kang, 2003; Choi, 2002; Choi and Park, 2002). Thus the time spent in the traditional process of structure optimization design for determining boundaries conditions could be reduced.

In this study, dynamic optimization of lower control arm of front double wishbone suspension was performed by combining the FMBD analysis and widely used structure optimization techniques through ESL method. After analysis of the new design after optimization, results revealed that the strength and stiffness of lower control arm were improved significantly, while the mass was almost unchanged. Moreover, the new design obtained from the results of dynamic optimization based on ESL method can satisfy the actual requirements of manufacturing process. In addition, structure dynamic optimization based on ESL method can avoid the dependency on personal experience, improve the accuracy of the optimal results, meanwhile decrease the time in product design.

### EQUIVALENT STATIC LOAD METHOD

**Equivalent static load:** According to the basic mechanic knowledge, the motion equations of the

structure under dynamic loads without taking friction into account can be expressed as:

$$M(b)\ddot{y}(t) + K(b)y(t) = F(t) \quad (1)$$

where,  $M(b)$  was the mass matrix,  $K(b)$  the stiffness matrix,  $y(t)$  the displacement vector,  $F(t)$  the external force vector. The Eq. (1) could be transformed into:

$$K(b)y(t) = F(t) - M(b)\ddot{y}(t) \quad (2)$$

which means that at moment  $t$ , the displacement of the structure  $y = y(t)$  could be regarded as combination result of the external and inertia forces. Assuming that there was a static load applied on the structure, which could generate the same displacements as  $y(t)$  in Eq. (2), the static load was named as the equivalent static load of dynamic load at that moment. Then Eq. (2) became:

$$F_{eq} = K(b)y(t) = F(t) - M(b)\ddot{y}(t) \quad (3)$$

**Optimization model:** Dividing the time history of the dynamic load into  $q$  constants, the equivalent static load  $F_{eq}^u$  can be obtained from Eq. (3) at any instant  $u_i$  ( $i = 1, 2, \dots, q$ ). So the optimization in continuous time domain could turn into solving optimization problems at a series of moments (Choi, 2002; Choi and Park, 2002):

$$\begin{aligned} & \min \varphi(b) \\ & \text{s.t. } K(b)y_u = F_{eq}^u \quad u = 1, 2, \dots, q \\ & g_{ju}(b, y_u, \dot{y}_u, \ddot{y}_u) \leq 0 \\ & j = 1, 2, \dots, m; u = 1, 2, \dots, q \end{aligned} \quad (4)$$

From equations above, it was obvious that the structural dynamic optimization based on equivalent static load method was basically the same with the traditional way. The only difference was that equivalent static load  $F_{eq}$  was introduced into the constraints instead of dynamic load. The process can be expressed as follows:

Start by setting  $p = 0$ ,  $b_p = b_0$ ;

Substitute  $b_p$  into Eq. (1) for transient analysis and calculate the equivalent static load:

$$F_{eq}^u = K(b_p)y_u \quad u = 1, 2, \dots, q \quad (5)$$

If  $p > 0$  and

$$\sum_{u=1}^q \|F_{eq}^u(p) - F_{eq}^u(p-1)\| < \epsilon \quad (6)$$

the optimization was completed. if not, turn to step.  $F_{eq}^u$  in Eq. (6) was the equivalent static load of the  $p$ -th iteration at moment  $u$ .

Solve the structural static optimization problem :

$$\min \varphi(b_{p+1}) \quad (7a)$$

$$\text{s.t. } K(b_{p+1})z_u = F_{eq}^u, \quad u = 1, 2, \dots, q \quad (7b)$$

$$g_{ju}(b_{p+1}, z_u) \leq 0, \quad j = 1, 2, \dots, m; u = 1, 2, \dots, q \quad (7c)$$

$$b_{p+1,kL} \leq b_{p+1,k} \leq b_{p+1,kU}, \quad k = 1, 2, \dots, n \quad (7d)$$

set  $p = p+1$ , turn to ②.

The objective function in Eq. (7) can be expressed as:

$$\varphi = c_0(b, T) + \int_0^T h_0(b, y(t), \dot{y}(t), t) dt \quad (8a)$$

and the constraint conditions were:

$$g_i = c_i(b, T) + \int_0^T h_i(b, y(t), \dot{y}(t), t) dt \begin{cases} = 0, & i = 1, \dots, p \\ \leq 0, & i = (p+1), \dots, m \end{cases} \quad (8b)$$

$$g_i = h_i(b, y(t), \dot{y}(t), t) \begin{cases} = 0, & i = (m+1), \dots, p \\ \leq 0, & i = (p+1), \dots, m \end{cases} \quad (8c)$$

In which  $c_0$  was the mass of the structure, the integral term was the response of displacement and strain. It can be seen that the constraint Eq. (8b) was not time-varied and the constraints, which could be displacement and stress, may change from Eq. (8c).

## FMBD ANALYSIS OF SUSPENSION

The front double-wishbone suspension studied in this study comprises: upper control arm, lower control arm, knuckle, shock absorbers, coil springs and tie rod *et al.* Taking the lower-arm as the objective of optimization, other parts were simplified to rigid bodies for they only guides the movement direction and transmits loads. Lower control arm was set up as a flexible body using finite element model according to its actual geometry. For further simplification of the FMBD model of front suspension, the bushings were

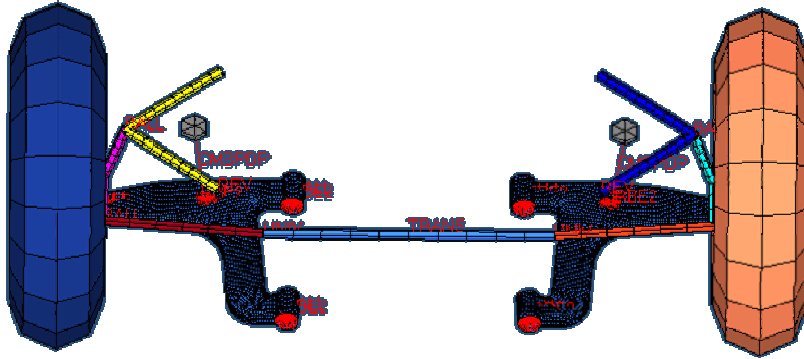


Fig. 1: The dynamic model of double wishbone for simulation

Table 1: Hard-point coordinates of left suspension

Hard point	X[mm]	Y[mm]	Z[mm]
Front point of UCA	-123	405	180
Rear point of UCA	176	405	154
Ball joint of UCA	26.5	605	167
Front point of LCA	-28.5	245	-73
Rear point of LCA	291.5	258	-73.5
Ball joint of LCA	-15	675.5	-95.5
Damper and Spring upper	43	458.5	186
Damper and Spring lower	-4	435	-68
Steering link inner	165	310	15
Steering link ball joint	120	650	0
Wheel center	0	750	0

Table 2: Material properties of lower-arm

Material	E[Gpa]	$\mu$	UTS	$\rho[\text{g/cm}^3]$
SAPH440	210	0.3	353	7.8

regarded as rigid motion pairs, and the springs and dampers were simplified as elastic damping elements. The elastic and damping effect of tires were simplified as flexible elements with six-degree freedom. The coordinate system was a right-hand orthogonal axis system, whose X-axis positive direction was from the rear to front of the car, the positive direction of Y-axis was from left to right and that of Z-axis was vertical upward. Appointing the origin of coordinate at middle of the two front wheel centers, hard-point coordinates of the left suspension were shown in Table 1.

The kinematic pair relations were the same as actual motion pairs. The FMBD model of front suspension was shown in Fig. 1 and the material properties were shown in Table 2.

Road conditions were: straight running on washboard road, steering on smooth road and steering on the large twisting road. The stress distribution of lower control arm and the reaction forces at motion pairs were shown in Fig. 2(a-f).

From the stress distribution of the lower-arm under three road conditions, it can be seen that the large stress

occurred at the connecting area of shock absorbers and the lower control arm. And the maximum stress exceeds the yield strength 353 MPa, as much as 433.2 MPa.

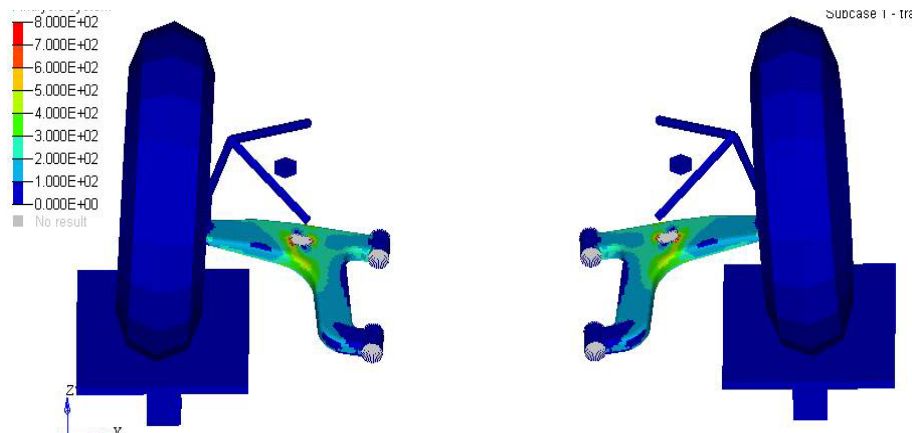
Therefore, the objective of optimization was to improve the strength and stiffness of lower-arm under different road conditions. From the varying force exerted on the lower control arm by motion pairs, it can be seen that the force at different joints reach the maximum value at different moment, as well as the force at different directions of the same motion pair reach maximum value at different moment. So some severe conditions may be omitted while carrying on structure optimization based on traditional methods, causing the strength of optimized structure cannot meet the requirements.

**Dynamic optimization:** As the control arm was a stamped part, adding draw-bead could significantly improve the strength and stiffness of it. So the optimal design of the lower-arm stress was focused on searching for the best distribution of the draw-bead on the arm. Then the structural optimization of lower-arm for draw-bead distribution could be described as:

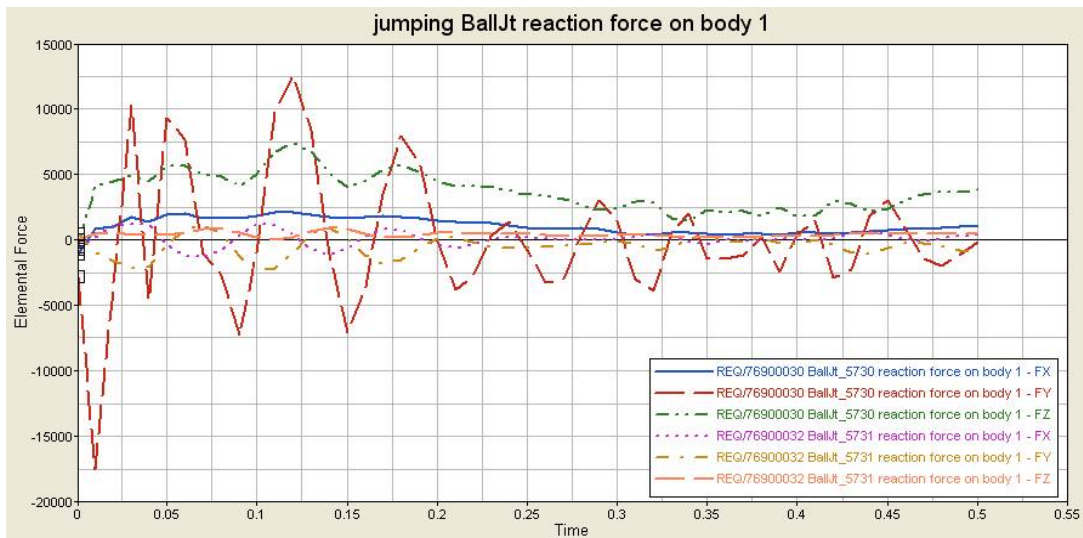
- **Design variables:** The entire lower-arm
- **Design objective:** Minimum flexibility
- **Constraint:** Draw-bead height  $h \leq 5$  mm

The optimization process reaches convergence after three loops. The stiffness has increased by 45.8% and the iterative course was shown in Fig. 3; the draw-bead distribution was shown in Fig. 4.

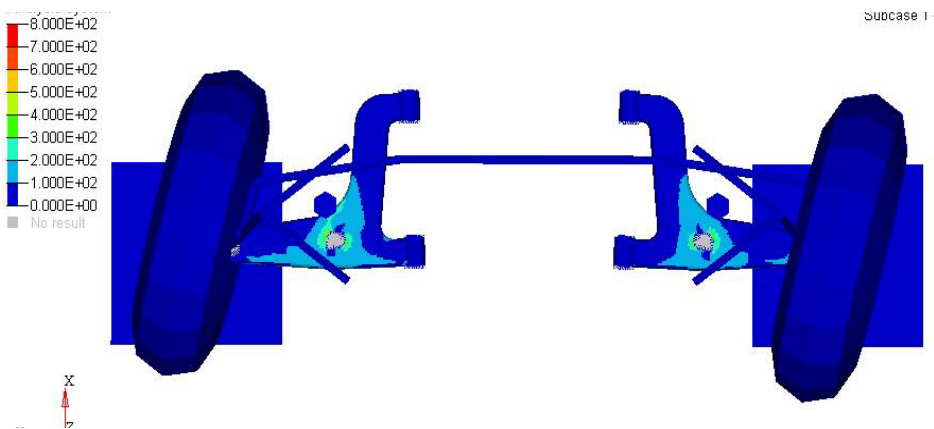
Multi-body dynamic model of the optimized lower-arm was set up to analyze its performance under the same working conditions for further comparisons. The stress distribution and the maximum value of the lower



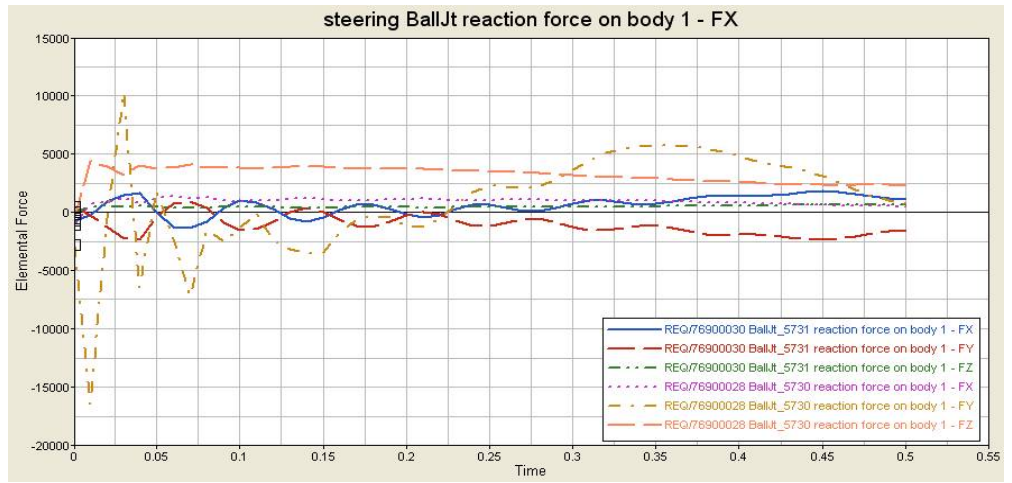
(a) Stress distribution on washboard road



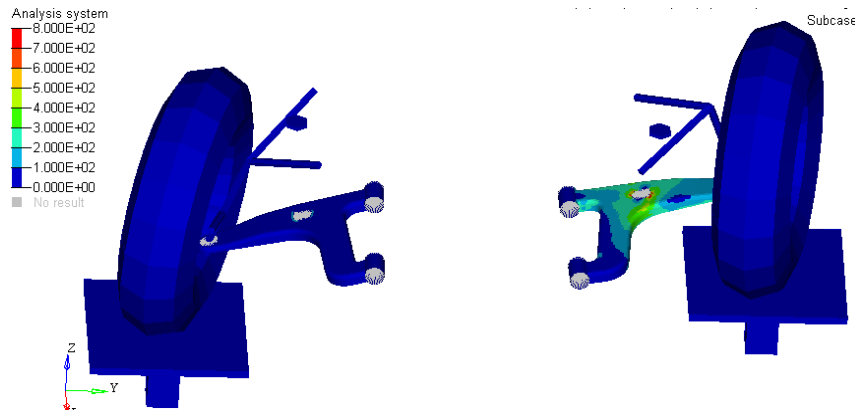
(b) Force on the lower-arm applied by car body



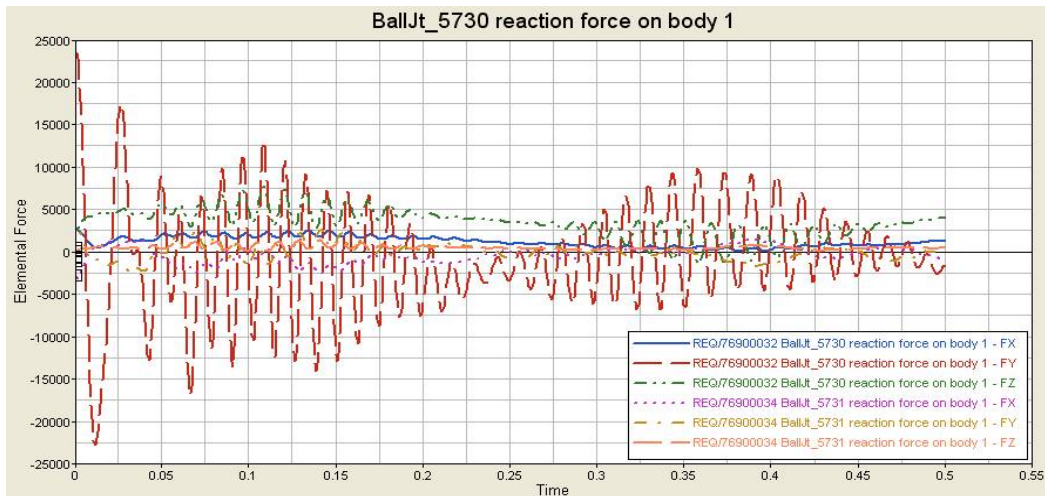
(c) Stress distribution while corning



(d) Forces on the lower-arm applied by car body



(e) Stress distribution while steering on twisting road



(f) Forces on the lower-arm applied by car body

Fig. 2: Stress distribution of the lower-arm and force-time history under different road conditions

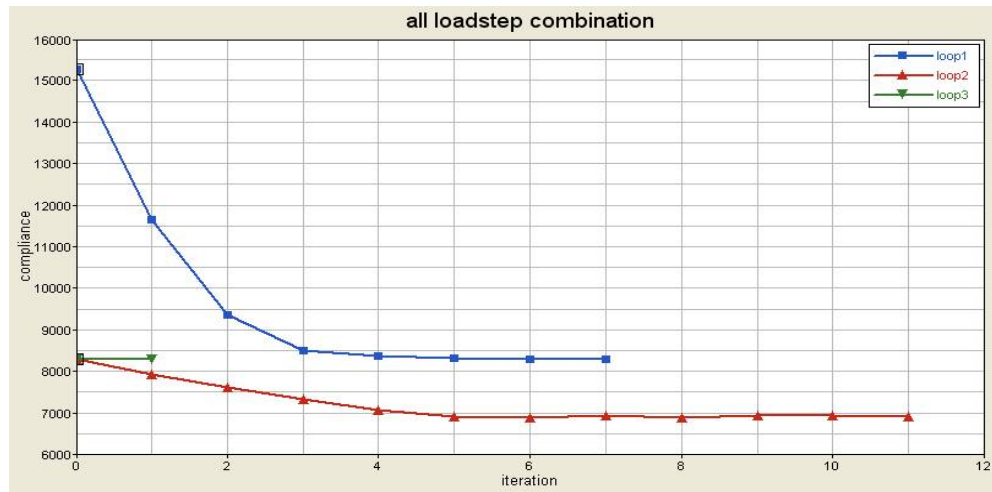


Fig. 3: The iterative course of the optimal objective function

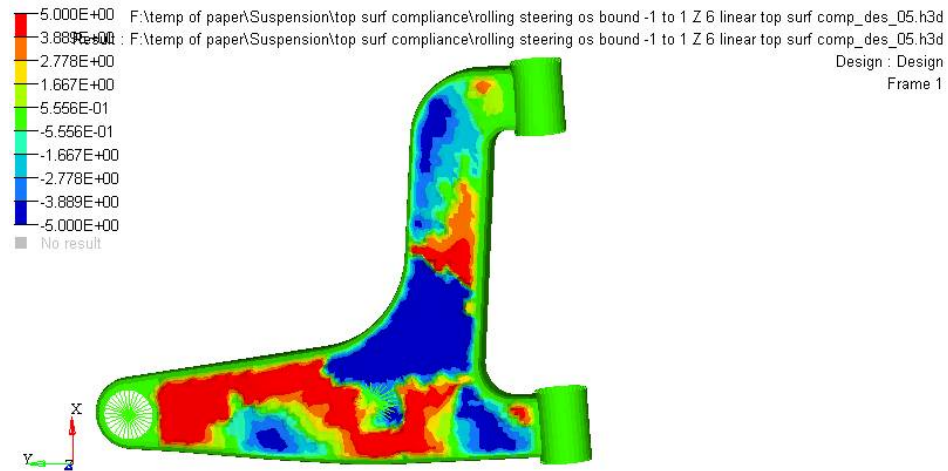


Fig. 4: Draw-bead distribution of lower-arm

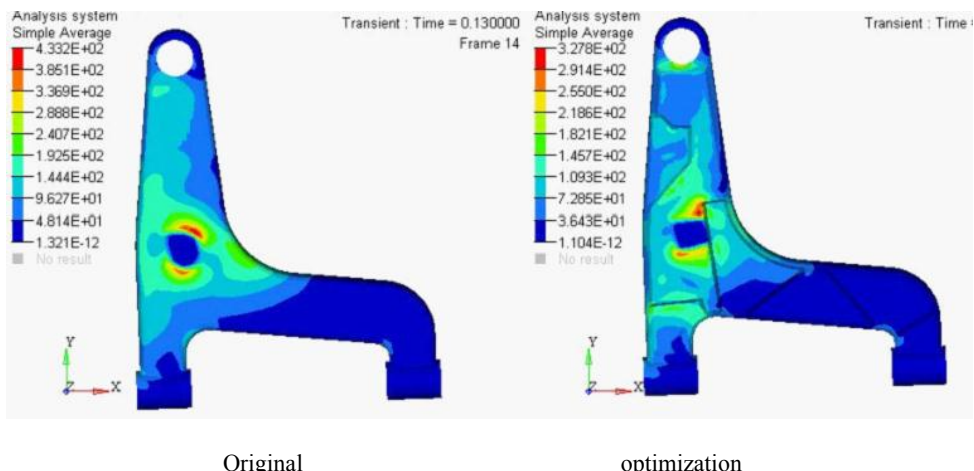


Fig. 5: Stress distribution of lower-arm before and after optimization

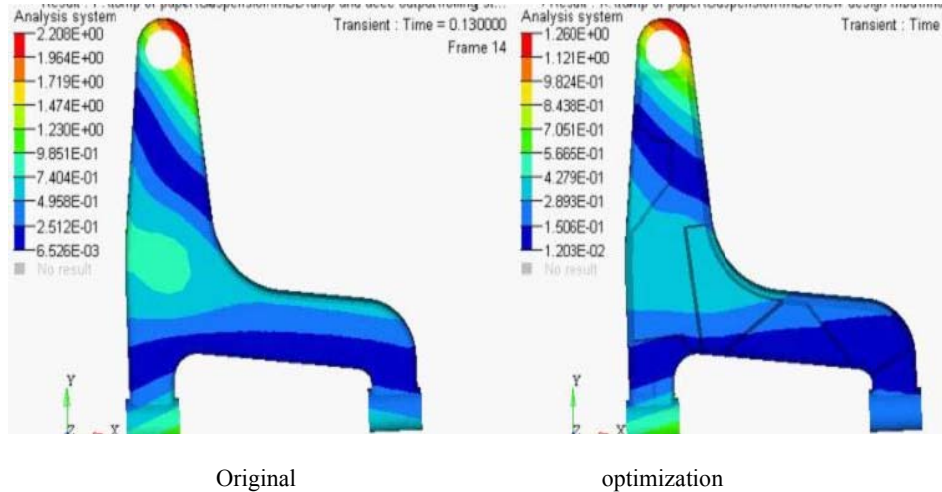


Fig. 6: Deformation of lower-arm

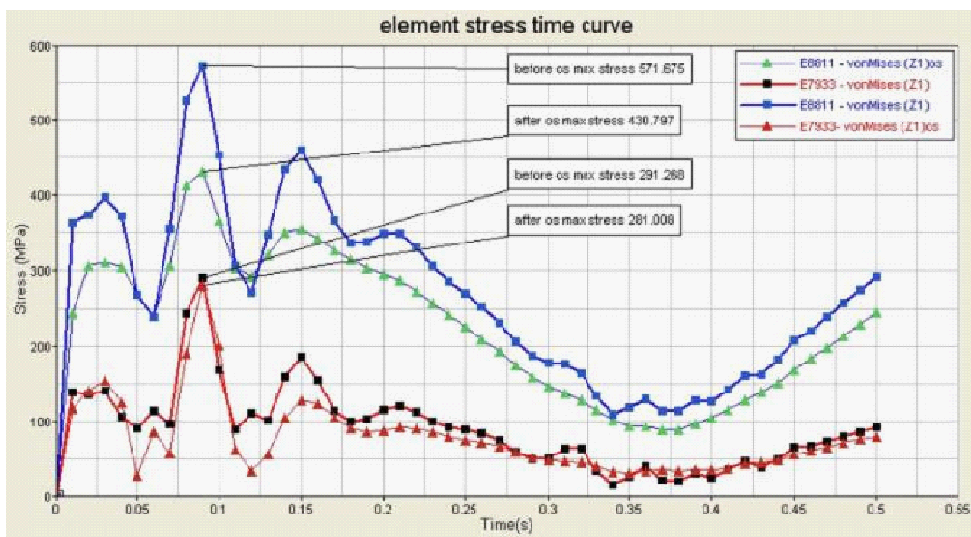


Fig. 7: Stress comparison of one grid before and after optimization

arm was shown in Fig. 5, while the deformation of the lower arm was shown in Fig. 6. Since the maximum stress happens at the areas around the joints that connect the lower arm to the shock absorber and to the body, two elements at the same location was selected and the stress time history of the two elements was shown in Fig. 7. The mass, stress and deformation of the lower arm before and after optimization was compared in Table 3.

From the results, it can be seen that the maximum stress on lower control arm under different road conditions was reduced from 433.2MPa to 327.8MPa after optimization, while the mass was increased only 5%, showing that the mechanical performance increased obviously.

Table 3: Change of lower control arm

	Original	Optimization	Change ratio
Maximum stress (MPa)	433.2	327.8	-24.3%
Deformation (mm)	2.208	1.260	-42.9%
Mass (Kg)	5.56	5.84	5%

Meanwhile the maximum deformation has reduced by 42.9%, from 2.208 to 1.26 mm.

## CONCLUSION

In this study, dynamic optimization of lower control arm of front double wishbone suspension was performed by combining the FMBD analysis and widely used structure optimization techniques through

ESL method. After analysis of the new design after optimization, results revealed that:

- The strength and stiffness of lower control arm were improved significantly, while the mass was almost unchanged.
- The new design obtained from the results of dynamic optimization based on ESL method can satisfy the actual requirements of manufacturing process.
- Structure dynamic optimization based on ESL method can avoid the dependency on personal experience, improve the accuracy of the optimal results, meanwhile decrease the time in product design.

#### **ACKNOWLEDGMENT**

This study was supported by the National High Technology Research and Development Program of China (2011AA11A265), the National Natural Science Foundation of China (50875173 and 51105241), the Key Project of Shanghai Science and Technology Commission (10JC1411600 and 11140502000), the Science and Technology Development Foundation of Shanghai Automotive Industry (1104) and the Natural Science Foundation of Shanghai (11ZR1414700).

#### **REFERENCES**

Choi, W.S., 2002. Transformation of Dynamic Loads into Equivalent Static Loads and Structural Optimization [D]. Hanyang University, Hanyang.

- Choi, W.S. and G.J. Park, 2002. Structural optimization using equivalent static loads at all the time intervals [J]. *Comput. Methods Appl. Mech. Eng.*, 191: 2105-2122.
- Fu, Y., 2009. Research on structural optimization design methods for suspension structure of vehicle with multiple loading conditions [J]. *Mach. Design Manuf.*, 25(8): 1-3.
- Kang, B.S., W.S. Choi and G.J. Park, 2001. Structural optimization under equivalent static loads transformed from dynamic loads based on displacement [J]. *Comput. Struct.*, 79(2):145-154.
- Lu, H., 2011. Lightweight design for rear suspension's upper arm of roewe750 [J]. *Mach. Design Res.*, 27(2): 111-113.
- Pan, X., 2007. Design optimization and fatigue live analysis for transmission mount bracket [J]. *Autom. Eng.*, 29(4): 341-345.
- Park, G.J. and B.S. Kang, 2003. Validation of a structural optimization algorithm transforming dynamic loads into equivalent static loads [J]. *J. Optim. Theor. Appl.*, 119(1): 191-200.
- Wang, F., 2009. A research on lightweight design for the lower-arm of suspension based on reliability theory [J]. *Autom. Eng.*, 31(11): 1071-1073.